

## INFN\_E/GEM4FUSION: GEM AND TIMEPIX BASED DIAGNOSTICS FOR MAGNETIC CONFINEMENT FUSION AND LASER PRODUCED PLASMAS

G. Claps<sup>1,2</sup> (Resp.), D. Pacella<sup>1,2</sup> (Ass.), F. Cordella<sup>2</sup>, V. De Leo<sup>2</sup>,  
D. Tagnani<sup>1</sup> (Tecn.), A. Tamburrino (Dott.)

*1 - INFN – Laboratori Nazionali di Frascati, via E. Fermi 54, 00044 Frascati, Italy*

*2 - ENEA FSN Department, C. R. Frascati, via E. Fermi 45, 00044 Frascati, Italy*

*Collaborations: CERN-European Organization for Nuclear Research (Switzerland), CNR-ISTP (Milano), Università Milano Bicocca, Université de Bordeaux (France)*

### 1 Introduction

Our research activity was born from a collaboration between ENEA and INFN in Frascati, and the following report outlines the main results obtained in this last year. Our work has been focused on four main research lines: test and calibration of a new GEMINI front-end electronics for  $10 \times 10$  cm<sup>2</sup> GEM detectors, measurements of the X-ray spectrum on a Laser Produced Plasma (LPP) with a side-on GEM detector, measurements of gamma emission on LPP with a Silicon Timepix3 detector and simulation studies for electronic shielding in high-flux radiation environments. The development of new front-end electronics arises from the need to protect electronics in high neutron flux environments, as expected on modern fusion reactors like the ITER tokamak. An agreement with the ITER diagnostic team has been signed to demonstrate that the GEM read-out electronics can be placed remotely. At the last year's end, this goal was reached, and now a new agreement is under approval. It envisages the realization of a new prototype GEM detector with this new front-end electronics and its tests with X-rays. Based on the accumulated work experience of these last years, a proposal for X-ray diagnostics on the new DDT Tokamak under construction at the ENEA Frascati research center has been submitted. Finally our group is also working on the characterization of Timepix-based detectors for the monitor of particles and neutrons, particularly on a new diamond detector based on Timepix3 for fast neutron detection on Tokamak. Details on this last activity that is interesting also in the framework of the INFN-E project can be found in the report of the n TOF experiment.

### 2 Characterization of the new GEMINI front-end electronics

Our GEM detectors cover an active area of  $10 \times 10$  cm<sup>2</sup>, with some alternatives that can be smaller ( $3 \times 3$  cm<sup>2</sup>) or bigger ( $20 \times 30$  cm<sup>2</sup>) depending on the specific applications. Regardless of their dimensions and applications, their layout follows a standard scheme that was tested and verified and is practically the same for all applications. Our GEM detectors are sealed chambers constituted by a cathode, three GEM foils and an anode. They have an input and output inlet

so that a specific gas mixture can flow inside. The gas layer between the cathode and the first GEM foil (the “drift region”) is the detector’s active volume and can be modified according to the specific application. Typically, its width is 3 mm, but this geometric parameter can be modified (fig. 1a). In general, the anode is divided into pads, and a dedicated read-out electronic is mounted on its backside to obtain the required info on the particle (fig. 1b).

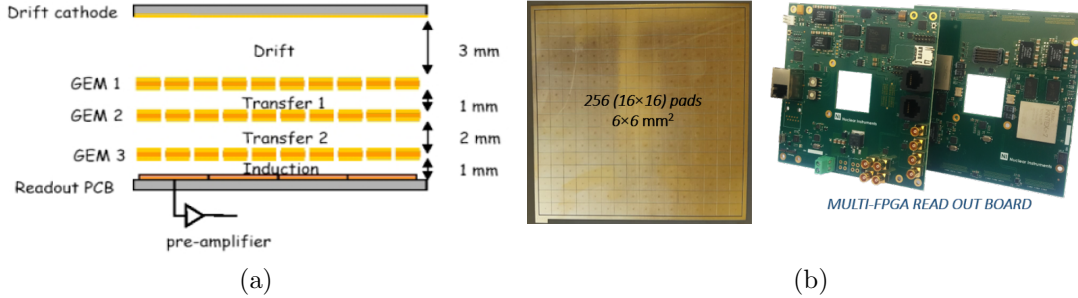


Figure 1: *a) Layout schema of a triple-GEM detector in one of the standard configuration with 3 mm of active gas layer and area of  $10 \times 10 \text{ cm}^2$ ; b) pads PCB with the main elements of read-out electronics: GEMINI chip cards and FPGA boards.*

The detector can be controlled through a multi-FPGA board developed by the Nuclear Instruments company. The main component of this new read-out electronic is the chip GEMINI (GEM INtegrated Interface). Its Architecture has been presented in previously published papers [1; 2]. The chip has been developed in  $0.18 \mu\text{m}$  C-MOS technology and can manage a maximum number of 64 channels, hence a maximum of 64 pads on the PCB anode. The main component of the GEMINI chip is a charge-sensitive preamplifier (CSP) with an open-loop gain of 64 dB and feedback capacitance. The role of CSP is to increase the amplitude of the current pulse signal coming from the pad and extend its time width. The signal is compared with a threshold level, and a 2 GHz internal clock begins to count when the pulse signal is over the threshold and stops when it returns under. This is the so-called Time-over-Threshold (ToT) mode, a widely used technique that allows a digitized charge measurement. Once a threshold level  $V_{T \text{ HR}}$  and a time constant  $\tau_F$  are fixed, ToT counts increase with the injected charge  $Q_{in}$ . Time is measured when the signal passes the threshold with a time resolution of up to 0.5 ns. A timestamp is registered for each hit. This provides the Time of Arrival (ToA) acquisition mode. For GEMINI chips, both threshold and feedback capacity can be tuned appropriately. The new front-end electronics are realized with a PCB pad board and 64D GEMINI cards (fig. 2) equipped with special connectors to insert micro-coaxial cable between them.

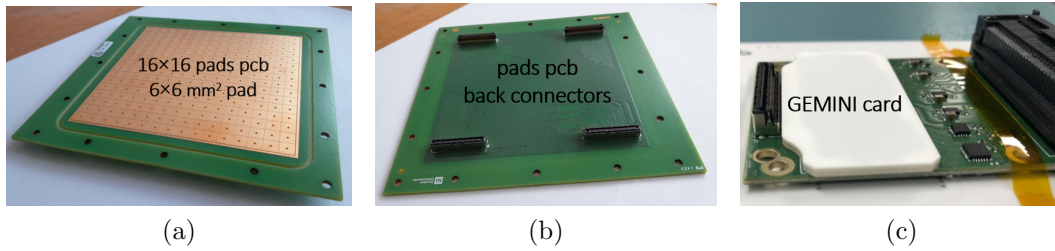


Figure 2: a)  $16 \times 16$  pad PCB board; b) the back side of the PCB board; c) a GEMINI card with 64 channels and samtec connector for micro-coaxial cables.

These components have also been realized by the Nuclear Instrument company, which provided cables of different lengths, from a minimum of 5 cm to a maximum of 2 m (fig. 3).

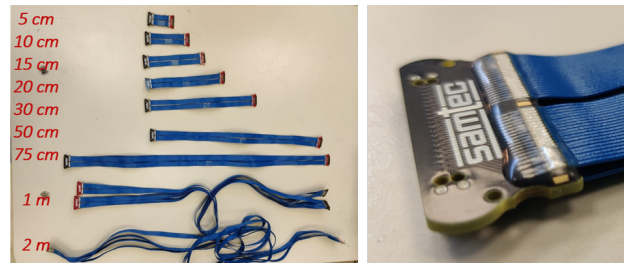


Figure 3: A photo of the Samtec cable with lengths from 5 cm to 2 m and a zoom on the cable connector.

To check the capability of these cables to transport signals in terms of noise and charge, we performed some experimental tests exciting the pad PCB with a square wave produced by a generator. The pcb board has been coupled to a GEM foil at a distance of 1 mm, and the square signal has been injected between the pcb board and the GEM electrode facing the pads (fig. 4). With this configuration, a signal is induced on pads at every falling edge of the square wave. This signal is similar to that induced by X-rays in a standard triple-GEM chamber. Then, it was possible to study the effect of these cables on the transported signals.

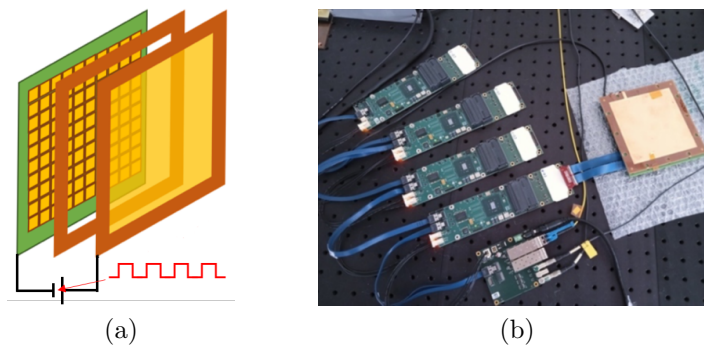


Figure 4: a) Layout of the pulser system realized by coupling the pads pcb with a GEM foil at a distance of 1 mm; b) a photo of the pulser system realized in the lab using only one 64D GEMINI card.

Our study focused on three main aspects: the determination of the minimum threshold value that ensures zero or negligible noise for each cable length, the signal resolution as a function of the cable length, and the dependence of signal resolution at different square wave amplitudes. In the first two cases, pad pcb was excited with a pulse frequency of 1 kHz and a wave amplitude of 10 V. Results are summarized in the plots of Fig. 5.

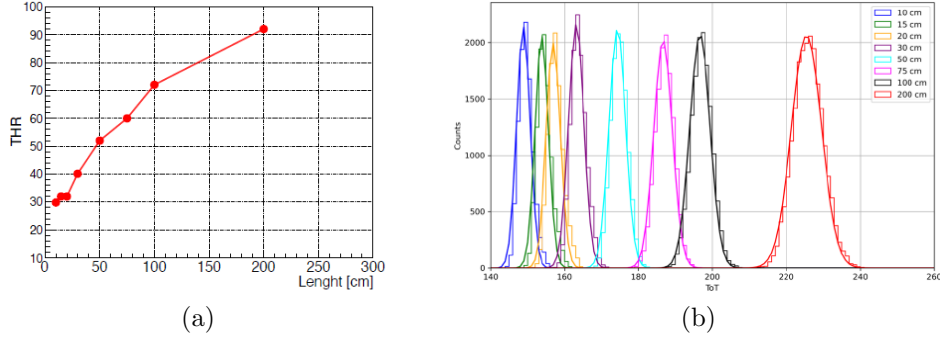


Figure 5: a) Minimum threshold values as a function of the cable length; b) ToT distributions obtained with increasing cable lengths.

As observed, when the cables are longer, the noise level rises, and higher threshold values must be set. At the same time, with longer cables, the measured mean values and the FWHM of the corresponding ToT distributions rise. This result was expected because the spread in time of signals gets worse over longer distances, especially at the maximum available length of 2 m. The third aspect was investigated using the 1 m cable and scanning the voltage amplitude from 1 V to 20 V with a step of 2 V (fig. 6).

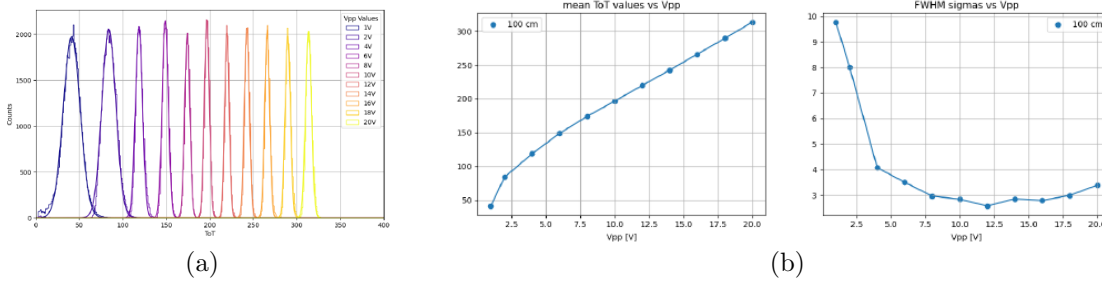


Figure 6: a) ToT distribution profiles as a function of the exciting signal amplitude; b) plot of the mean and FWHM of the ToT distributions as a function of the exciting signal amplitude.

The response of the mean Time-over-Threshold (ToT) value, derived from a Gaussian fit applied to the signal voltage, mirrors the expected parameter in calibration curves, including the non-linear part associated with low signal amplitudes. The signal resolution demonstrates enhancement as the applied voltage increases, reaching a minimum point at a signal amplitude of 12 V. All these results demonstrate that the remotization of read-out electronics can be realized by obtaining a satisfying signal transport with cables at least 1 m long.

### 3 The new side-on GEM detector

The idea of realizing a new GEM detector in a side-on configuration arises from the need to make charge measurements on the X emission from laser plasma (fig. 7). Typically, X-ray emission from these sources lasts for few tens of ps and X-ray photons cannot be measured separately. Since the new electronics can perform charge measurements, this new detector has been conceived to estimate the X-ray spectrum from charge measurements. The following paragraph will outline the results obtained on the ILIL laser facility at the CNR-Istituto Nazionale di Ottica (CNR-INO) in Pisa. The used GEM detector is based on standard  $10 \times 10 \text{ cm}^2$  GEM foils with the usual 1, 2, and 1 mm gaps. The region between the cathode and the first GEM foil is 12 mm thick and has an entrance and exit window of  $6 \times 80 \text{ mm}^2$ .

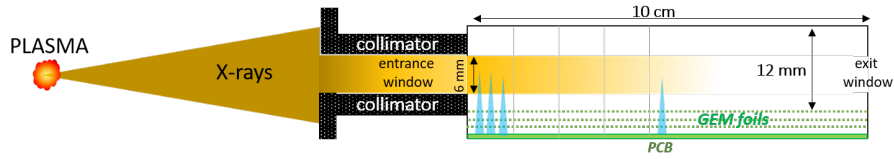


Figure 7: *Layout schema of the side-on triple-GEM detector with 12 mm of active gas layer and  $10 \times 10 \text{ cm}^2$  area.*

The PCB anode is divided into four lines of 64 pads, each one having an area of  $1.5 \times 20 \text{ mm}^2$  (fig. 8a). Then all the gas in 96 mm deep can be exploited to measure the absorption profiles (fig. 8b). The charge collected from a single pad is due to the piled-up charge released by bursts of photons that interact in the overlying gas layer. This configuration can be helpful to measurements on hard-X ray photons because the gas layer now extends 10 cm.

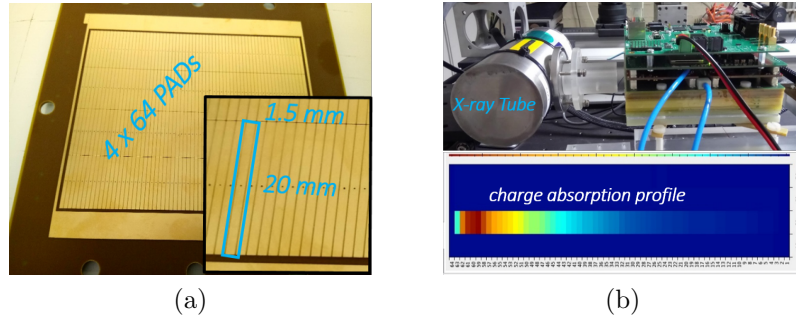


Figure 8: *a) A photo of the pad's PCB layout; b) A measure of the absorption profile obtained in the NIXT lab with an X-ray tube.*

This GEM detector in side-on configuration exploits a principle similar to the Bremsstrahlung cannon [3; 4; 5] but is limited to X-ray spectra until 30-40 keV. The idea behind this type of measurement is to derive the X-ray spectrum from transmission measurements, a method consolidated in other fields of application. To improve the subsequent mathematical treatment, the experimental measure of the transmission profiles must reach the right level of accuracy [6].

#### 4 Profile measurements at the CNR-INO laser facility

First measurements of the X-rays emission from a laser plasma have been performed on the laser facility at the CNR-INO research center. The used laser is a Ti:Sa CPA (Chirped Pulse Amplification) that can reach a power of 240 TW and a pulse duration of a few tens of fs. In the past, we participated in an experiment designed to accelerate protons. During the last year, we participated in two experimental campaigns: one was optimized for our needs to test the GEM detector response to different solid state targets, the second was dedicated to the nano-structured targets and the X-ray acquisition of our systems was parasitic. The material targets used during the first campaign were thin sheets of Ti, Al, Cu, and Mylar. The GEM detector was installed out in air in front of a port placed on the same side of the incident laser (fig. 9a) and was equipped with a pin-hole of 0.9 mm. To screen the detector electronics from the electromagnetic pulse (EMP) disturbance, it was covered with an Aluminum case with only two openings at the detector windows (fig. 9b). On the back side window of the Aluminum case, a Silicon Timepix3 detector was installed in side-on configuration. It is a thickness of 1 mm and has been conceived to measure gamma photons, as shown in the next paragraph.

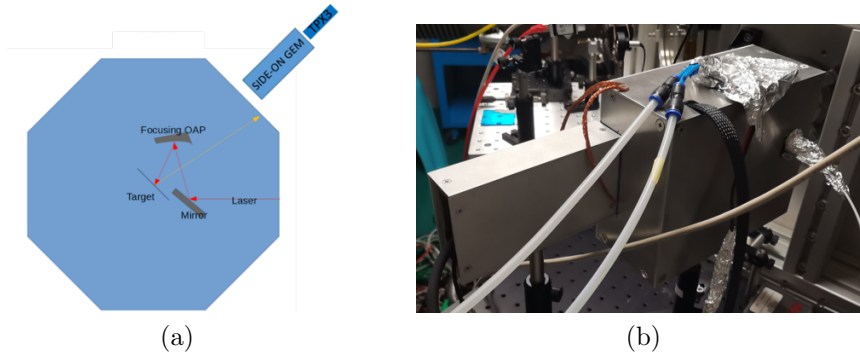


Figure 9: *a) Layout of the interaction chamber of the ILIL laser with a scheme of the installed GEM and Timepix3 detectors; b) A photo of the diagnostic system installed on the port of the interaction chamber: it is possible to distinguish the two detectors installed in sequence.*

For the measurements of the absorption profiles, only one row of pads was used, reducing the entrance window on the Aluminum box. Each pad measures the charge released by a multi-photon interaction at a given depth in the gas. Fig. 10 shows the measured absorption profiles obtained with a single laser shot on the different target materials.

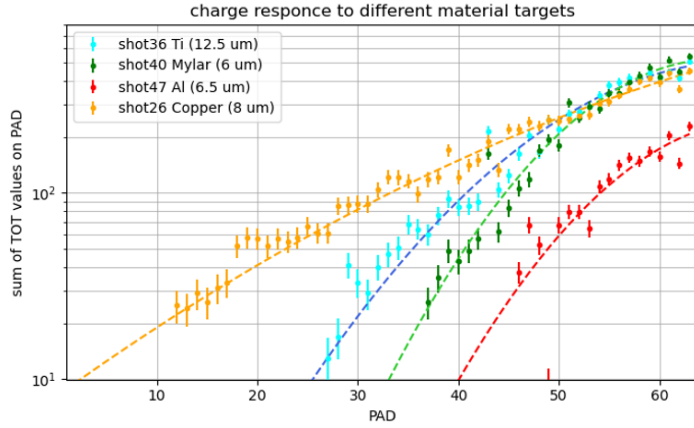


Figure 10: Measured X-rays absorption profiles on different target materials (in ToT units).

According to the physics of the laser-target interaction, the X-ray emission comes from two contributions: the Bremsstrahlung of the accelerated electrons inside plasma that reach the solid target and, in the case of metals, the  $k\alpha$  line. To estimate the reliability level of the profile measurements, the absorption profiles have been simulated through the FLUKA MC code, inserting monochromatic X-ray lines and compared to the measured profiles. Simulations also consider that the detector works in air and then the original spectrum is attenuated by the Kapton window of the vacuum interaction chamber, the air gap, and the  $15 \mu\text{m}$  thick Kapton window of the detector itself. Fig. 11 shows some measured profiles on Ti targets and compares one of these with simulated profiles coming from monochromatic X-ray lines.

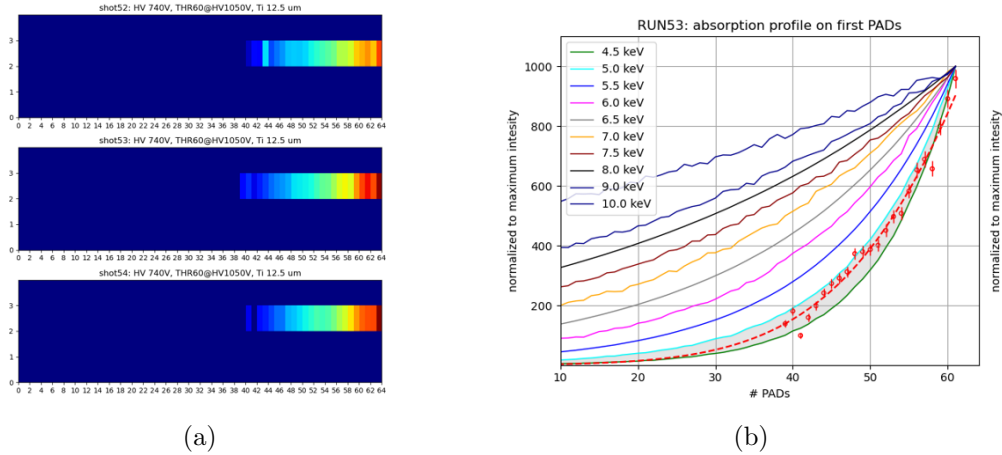


Figure 11: a) 2D profiles obtained after three shots on  $5 \mu\text{Ti}$  targets with the same laser focus; all the profiles are consistent with each other; b) Comparison of the central shot profile with monochromatic as obtained with MC Fluka simulations.

The measured profiles on a given target are reproducible, and the comparison of monochromatic profiles shows that the contribution comes mainly from the the  $k\alpha$  lines. In addition, for



some shots, the observed uncertainties are confined to 0.5 keV. This represents an encouraging result towards optimizing the absorption profiles needed to reconstruct the X-ray spectrum of laser-induced plasmas.

## 5 Gamma rays diagnostic with a side-on Silicon Timepix3 detector

In recent years, a simple method to estimate the gamma energies from laser-produced plasmas has been developed. It was based on a Silicon Timepix detector in a side-on configuration. Despite its thickness of only 300  $\mu\text{m}$ , it was possible to identify the characteristic tracks from the interaction of Compton electrons produced by gamma interaction. Then, by evaluating the energy released by these electrons, it was possible to estimate the gamma energies in a range from 1 to 3 MeV with uncertainties of less than 0.25 MeV [7]. Recently, this diagnostic system has been upgraded using a Silicon Timepix3 detector with a thickness of 1 mm. It was installed immediately after the GEM chamber on the ILIL laser facility to extend the diagnostic system to gamma rays (fig. 12).

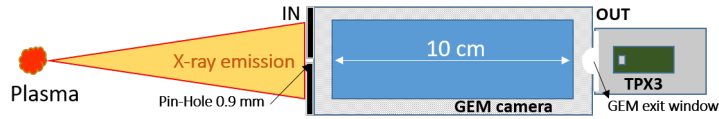


Figure 12: *Layout schema of the TPX3 set-up with the side-on GEM chamber placed before the Timepix3.*

The control module of Timepix3 was placed remotely through a dedicated cable. This arrangement was required to ensure the correct functionality of the read-out electronics affected by the EMP as demonstrated in previous tests. To obtain energy estimation, this new Timepix3 has been first calibrated with established gamma emission sources:  $^{55}\text{Fe}$ ,  $^{133}\text{Ba}$ ,  $^{109}\text{Cd}$ ,  $^{57}\text{Co}$ ,  $^{57}\text{Co}$  and  $^{137}\text{Cs}$ . Fig. 13 shows the calibration spectra in ToT units as obtained after an appropriate cluster analysis.

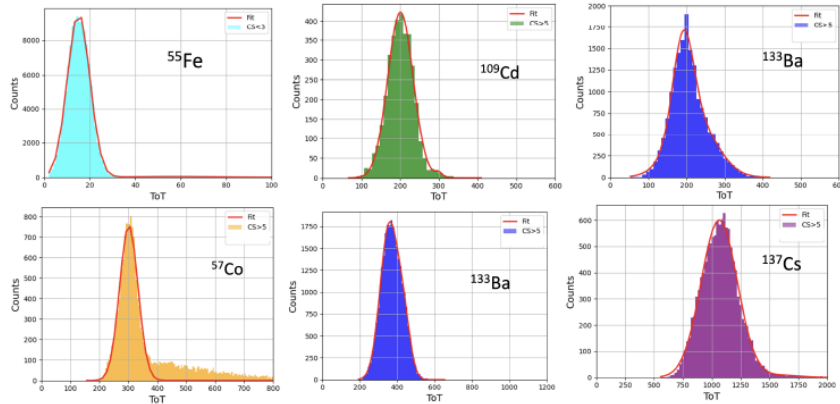


Figure 13: *ToT distribution obtained with different laboratory sources after tracks analysis.*



The morphological analysis on the detected tracks was performed by using several key parameters, including ToT volume (ToT), cluster size (CS), cluster height (CH), linearity (LIN), and roundness (RND). We refer to the publication of V. De Leo for their definition and the relative track analysis. Then, the track analysis was applied to data obtained from the laser plasma experiment by integrating all the significant shots to have sufficient statistics. Results are outlined in the plot of fig. 14.

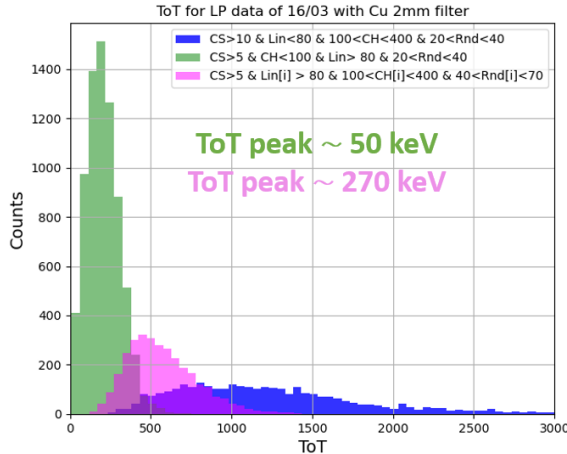


Figure 14: *Distributions identified considering the morphological analysis of the tracks studied during the calibration procedure.*

As can be observed, applying appropriate cuts on the acquired cluster made it possible to identify at least two peaks in the gamma region at energies of about 50 keV and 270 keV, respectively. This Timepix3 detector, and the side-on GEM detector offers a compact diagnostic system that can cover a photon range from soft-X rays to hard-X and gamma. Its spectral sensitivity, especially with TPX3, is limited but is one of the few diagnostics that can provide spectroscopic info in a quick and reliable way on laser produced plasma sources.

## 6 Shielding studies with MC simulations

An innovative framework that enhanced radiation shielding efficiency was introduced using a genetic algorithm with dynamic penalties and a bespoke parallel computing architecture. An illustrative case study centers on minimizing the Total Ionizing Dose for a silicon slab, focusing solely on the layer number and total thickness, with the potential for integrating additional constraints such as cost and density (fig. 15).

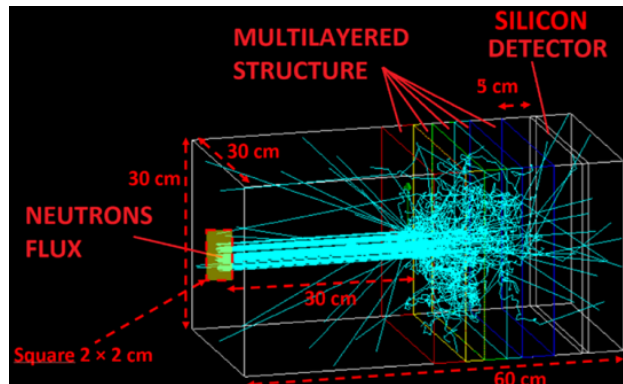


Figure 15: *Geant4* simulation of a beam of parallel 14 MeV neutrons (color aqua) impinging on a multi-layer shield (from red to blue color) protecting a silicon slab (gray color) simulating a detector. The snapshot was drawn using the OpenGL library with 100 impinging neutrons.

Integrating the genetic algorithm with Geant4 simulations within a customized parallel computing architecture demonstrates the convergence of Total Ionizing Dose values. To mitigate genetic algorithm challenges, including premature convergence and imperfectly tuned search parameters, a Total Ionizing Dose Database Vault object is introduced to expedite search speed (via data persistence) and maintain detailed information about all solutions independently. Analysis conducted using the Total Ionizing Dose Database Vault underscores boron carbide as the optimal material for the initial layer for neutron shielding, with high-Z materials (e.g. Tungsten) recommended for subsequent layers to halt secondary gammas. A validation comparison between Geant4 and MCNP under specific simulation conditions is performed. The benefits of the bespoke parallel computing architecture outlined herein encompass resilience, scalability, autonomy, flexibility, and efficiency, resulting in significant computational time savings. The proposed genetic algorithm-based methodology efficiently optimizes radiation shielding materials and configurations, with potential applications spanning space exploration, medical devices, nuclear facilities, radioactive sources, and radiogenic devices. For further details, we refer to the publication of F. Cordella.

## 7 List of Conference Talks by LNF Authors in Year 2023

1. V. De Leo, Advancing Plasma Analysis: An Integrated X-ray Spectroscopy System Utilizing GEM and Timepix3 Technology for Soft and Hard X-Rays, and Gamma Radiation Detection, High Precision X-Ray Measurements workshop, INFN - Laboratori Nazionali di Frascati, 19–23 June 2023
2. A. Tamburrino, Rivelatore Timepix3 per la misura dei prodotti di decadimento del radon, XXXVIII Congresso Nazionale Airp, Milano, 28–30 settembre 2022

## 8 Publications

List of papers published by Frascati INFN\_E members in 2023:

1. A. Tamburrino, G. Claps, G.M. Contessa, A. Pietropaolo, F. Cordella, V. De Leo, R.M. Montereali, M.A. Vincenti, V. Nigro, R. Gatto, D. Pacella, Thermal neutron detection by means of Timepix3, *Eur. Phys. J. Plus*, vol. 138, no. 11, p. 988, 2023, doi: 10.1140/epjp/s13360-023-04583-0
2. F. Cordella, M. Cappelli, M. Ciotti, G. Claps, V. De Leo, C. Mazzotta, D. Pacella, A. Tamburrino, F. Panza, Genetic algorithm for multilayer shield optimization with a custom parallel computing architecture, *Eur. Phys. J. Plus*, 2024, doi: 10.1140/epjp/s13360-023-04842-0
3. V. De Leo, G. Claps, F. Cordella, G. Cristoforetti, L.A. Gizzi, P. Koester, D. Pacella, A. Tamburrino, “Combined Spectroscopy System Utilizing Gas Electron Multiplier and Timepix3 Technology for Laser Plasma Experiments,” *Condens. Matter*, vol. 8, no. 4, 2023, doi: 10.3390/condmat8040098.
4. S. Cesaroni, F. Bombarda, S. Bollanti, C. Cianfarani, G. Claps, F. Cordella, F. Flora, M. Marinelli, L. Mezi, E. Milani, D. Murra, D. Pacella, S. Palomba, C. Verona, G. Verona-Rinati, Conceptual design of CVD diamond tomography systems for fusion devices, *Fusion Engineering and Design*, Volume 197 December 2023, Article number 114037, doi: 10.1016/j.fusengdes.2023.114037

## References

1. A. Pezzotta, G. Corradi, G. Croci, M. De Matteis, F. Murtas, G. Gorini, A. Baschiroto, GEMINI: A triple-GEM detector read-out mixed-signal ASIC in 180nm CMOS, in 2015 IEEE International Symposium on Circuits and Systems (ISCAS) (2015), pp. 1718–1721
2. A. Muraro et al., Development and characterization of a new soft x-ray diagnostic concept for tokamaks, *Journal of Instrumentation*, Volume 14, Article number C08012 (2019)
3. C. D. Chen, J. A. King, M. H. Key, et al., A Bremsstrahlung spectrometer using k-edge and differential filters with image plate dosimeters, *Rev. Sci. Instrum.* 79, 10E305 (2008)
4. A. Hannasch et al., Compact spectroscopy of keV to MeV X-rays from a laser wakefield accelerator, *Sci Rep* 11, 14368 (2021)
5. P. Koester, F. Baffigi, G. Cristoforetti, et al., Bremsstrahlung cannon design for shock ignition relevant regime, *Rev. Sci. Instrum.* 92, 013501 (2021)
6. E. Y. Sidky et al., A robust method of x-ray source spectrum estimation from transmission measurements: Demonstrated on computer simulated, scatter-free transmission data, *J. Appl. Phys.* 97, 124701 (2005)

- 7 . G. Claps et al., Timepix3 detector and Geant4-based simulations for gamma energy detection in Laser Produced Plasmas, JINST, Volume 14, Issue 92 September 2019 Article number P09005